AD_____

Award Number: DAMD17-03-1-0743

TITLE: Acoustic Emission Based Surveillance System for Prediction of Stress Fractures

PRINCIPAL INVESTIGATOR: Ozan Akkus, Ph.D.
Nicholas Wasserman

CONTRACTING ORGANIZATION: The University of Toledo
Toledo, OH 43606-3390

REPORT DATE: September 2005

TYPE OF REPORT: Annual

PREPARED FOR: U.S. Army Medical Research and Materiel Command
Fort Detrick, Maryland 21702-5012

DISTRIBUTION STATEMENT: Approved for Public Release;
Distribution Unlimited

REPORT DOCUMENTATION PAGE

Form Approved
OMB No. 0704-0188

1. REPORT DATE *(DD-MM-YYYY)*	2. REPORT TYPE	3. DATES COVERED *(From - To)*
01-09-2005	Annual	1 Sep 04 – 31 Aug 05

4. TITLE AND SUBTITLE
Acoustic Emission Based Surveillance System for Prediction of Stress Fractures

5a. CONTRACT NUMBER

5b. GRANT NUMBER
DAMD17-03-1-0743

5c. PROGRAM ELEMENT NUMBER

6. AUTHOR(S)
Ozan Akkus, Ph.D.
Nicholas Wasserman

E-Mail: ozan.akkus@utoledo.edu

5d. PROJECT NUMBER

5e. TASK NUMBER

5f. WORK UNIT NUMBER

7. PERFORMING ORGANIZATION NAME(S) AND ADDRESS(ES)
The University of Toledo
Toledo, OH 43606-3390

8. PERFORMING ORGANIZATION REPORT NUMBER

9. SPONSORING / MONITORING AGENCY NAME(S) AND ADDRESS(ES)
U.S. Army Medical Research and Materiel Command
Fort Detrick, Maryland 21702-5012

10. SPONSOR/MONITOR'S ACRONYM(S)

11. SPONSOR/MONITOR'S REPORT NUMBER(S)

12. DISTRIBUTION / AVAILABILITY STATEMENT
Approved for Public Release; Distribution Unlimited

13. SUPPLEMENTARY NOTES

14. ABSTRACT

Stress fractures of bone constitute the most serious musculoskeletal overuse injury during military training of male and female recruits. We believe that the cascade of events in stress fractures is structured as the upregulation of bone turnover, amplification of porosity, induction of greater local strains and associated increase in damage activity a priori to fracture. The hypothesis of our study is that the onset of stress fractures can be predicted by monitoring the evolution of microdamage activity using acoustic emissions. During the first year bone tissue was procured and amassed for specimen preparation. A sufficient number of donor tibias have been obtained and have been machined into test specimens. The test system was redesigned after the first year to improve the performance of both the mechanical testing as well as the acoustic emission detection of microdamage events. Different groups of beams will be tested to varying degrees of mechanical property degradation and histological examination will be used to determine the relationship between the acoustic event parameters and the microdamage morphology. The first group of beams are to be tested in fatigue until failure and these tests are currently underway.

15. SUBJECT TERMS
No subject terms provided.

16. SECURITY CLASSIFICATION OF:			17. LIMITATION OF ABSTRACT	18. NUMBER OF PAGES	19a. NAME OF RESPONSIBLE PERSON
a. REPORT	b. ABSTRACT	c. THIS PAGE			USAMRMC
U	U	U	UU	21	19b. TELEPHONE NUMBER *(include area code)*

Table of Contents

INTRODUCTION

The overall hypothesis driving this work was that an increase in microdamage activity during repeated loading of bone will signal the approaching stress fracture. Interception with the training regime prior to the incidence of the fracture as signaled by acoustic emissions would reduce the time necessary for recuperation and it would increases the preparedness and effectiveness of military personnel consequently. In order to test this hypothesis, fresh-frozen human tibias from males and females between the ages of 20 and 50 years old have been acquired for use in testing procedure outlined below. Sections of the tibias have been removed and machined into a proper geometry for fatigue tests. The formation and propagation of microdamage, in the form of microcracks and diffuse damage, produces detectable acoustic emission events similar to the seismic motions of an earthquake. Microdamage formation with characteristic waveform properties is being monitored through the use of piezoelectric acoustic emission transducers. Following the completion of fatigue testing, histological stains will be used to label the microdamage present in the samples prior to and after fatigue testing to quantify the amount and morphology of the damage in order to develop relationships between the histological parameters and acoustic emission parameters. These relationships will be used to identify the acoustic emission parameters that are best able to predict the total score of damage.

BODY

There are three primary objectives in this study. During the first two years, it is planned to 1) determine the characteristics of damage events that signal the onset of stress fractures and 2) quantify the differences between genders on the evolution of fatigue damage. These two objectives will be accomplished concurrently during the first two years of the project. Attainment of these aims requires:

a) Preparation of specimens from male and female tibias
b) Mechanical induction of fatigue damage within these specimens through fatigue tests
c) Monitoring microcracks using acoustic emission technique in real-time during fatigue loading
d) Histological characterization of damage amount and damage morphology
e) Analysis of the data obtained from above tests.

The last primary objective of this work is to 3) investigate and quantify the damage events during the *in vitro* fatigue of whole bone stress fracture model. This third objective requires the completion of the first two and is planned to proceed in the third year. The following will detail the progress made toward achieving the first two objectives during the first year of the study.

Procurement of Tibias and Specimen Preparation

Step a) requires the collection of donor tibias from males and femaleS from an age group relevant to military recruits. Since the focus of this work is the fatigue/fracture properties of those likely to be subjected to the rigors of military training, we needed to restrain our donor pool to a relevant age range. We initially specified an age range between 18 and 30 years old to various tissue collection agencies (NDRI, MTF, IIAM); however, the range was redefined as 18-50 years-old due to the limited number of donors available within the former age range.

Since September of 2003 we have received tibias from nine male donors (aged between 22 and 52 years old) and seven females (aged between 19 and 49 years old). Seven of the male donors and four of the female donors provided both tibias to this study bringing our total number of tibias available to 27, which is sufficient to complete the study.

Mechanical Testing Hardware and Test Setup

We initially chose to use a four point bending test configuration in order to induce the fatigue damage to the specimens due to this configuration's ability to subject the specimens to both tensile and compressive loading

modes, which reflects the complicated *in vivo* loads experienced by bones more effectively than uniaxial testing. The preliminary fatigue tests revealed that some samples demonstrated an increasing stiffness with increasing number of loading cycles. Such behavior is not a natural characteristic of bone's fatigue but it is the outcome of wear of the specimens at locations in contact with loading and support shafts (*1*). While steps were taken to resolve this issue (see Year 1 Report), the problem persisted despite various attempts to stabilize the test setup and reduce wear. We decided to proceed using a three-point bending setup (Appendix A). The primary difference between three and four point bending is that under three point bending, shear stresses are generated directly beneath the upper loading point. Preliminary testing with the three point bending setup showed the expected decrease in stiffness during fatigue loading in a consistent manner, thus justifying its substitute for four-point bending. Due to the length of time necessary to carry out the fatigue test (~ 5-14 hours), specimens are kept hydrated in a saline solution supplemented with $CaCl_2$ and protease inhibitors to prevent the degradation of the tissue's mechanical properties through mineral leaching and protein denaturation. The three-point bending fixtures (Appendix A) utilize a drip mechanism, a solution reservoir, and a pump in order to circulate the previously used solution back into the reservoir, reducing the amount of solution needed to perform the tests.

The fatigue testing is being conducted under load-controlled conditions and uses the decrease in specimen stiffness as a measure of test progress. In order to calculate the change in compliance a commercial displacement gage (Epsilon Technology Corp., Jackson, WY) was modified with an extension which allowed the gage to be placed well away from the specimen/solution and provide a more accurate measure of the sample's displacement at the mid-span, rather than having to rely on the system's actuator.

Preliminary testing of the three-point bending system was conducted using spare beams previously machined from femurs (n = 5) under the loading regime described in the proposal. This regime uses a high strain rate loading regime, which uses a rapid loading and unloading rate (as would be experienced *in vivo*) that repeats at a frequency of 2 Hz (Figure 1). The degradation of the specimens' mechanical properties were monitored by measuring their stiffness (Δ load / Δ displacement) during the test. These stiffness curves were rather noisy (Figure 2) and the knee-region of the curves were inconsistent. Since we are planning to stop the fatigue tests at different levels of specimen degradation, this is a problem because we were hoping to use the stiffness curve as a guide for when to stop the tests. We determined that the cause of this problem to be the loading regime. Beams machined from tibias were tested under a sinusoidal loading regime (Figure 1) displayed consistent and smooth stiffness degradation curves in comparison to the high strain rate loading regime. The sinusoidal loading, while not strictly representative of the *in vivo* conditions is a standard test method commonly used in the literature (*2-4*). More importantly, it provides us with the ability to consistently stop the tests at pre-determined levels of degradation. We plan to use four groups: total failure (Group I), pre-knee (Group II), mid-knee (Group III), and post-knee (Group IV) (Figure 2). The membership of the specimens into the four groups has been performed in such a way as to balance the test between age, sex, and anatomical location from where the beam was produced (anterior-medial, posterior-medial, lateral, or posterior). Appendix B provides details of the specimens in each group.

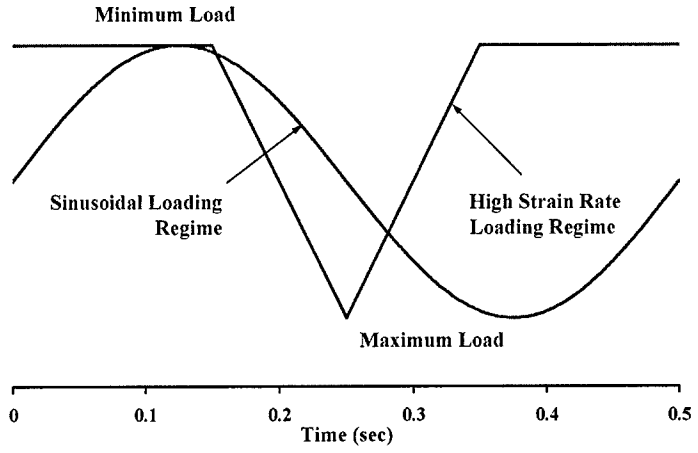

Figure 1: High strain rate (red) and sinusoidal (black) loading curves

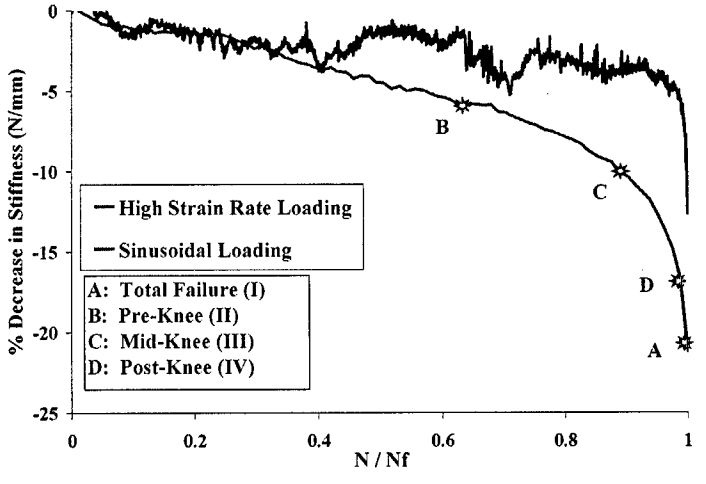

Figure 2: Compliance curves for high strain rate (red) and sinusoidal (black) loading curves. The points along the compliance curve labeled A-D represent the different pre-determined levels of degradation at which the tests will be stopped.

Monitoring Microcracks Using Acoustic Emission

The next step in the experimental setup was to setup the acoustic emission (AE) detection system. This system consists of two acoustic emission transducers, two signal amplifiers and a computer which analyzes and stores the AE data. The amplifiers, computer control board and software were acquired prior to the beginning of this study.

While conducting the four point bending tests, the transducers were mounted to the specimen using cyanoacrylate glue at the bounds of the inner mid-span region. Before the conclusion of preliminary four point bending test, we noticed that the transducers were not very durable under our testing conditions and they had failed on multiple occasions from either user-handling or from environmental corrosion. The new three-point bending setup allowed the use of more rugged transducers which are mounted to the outer supports of the test fixtures (Appendix A) using vacuum grease. During feasibility testing of the three point setup, we noticed that noise generated by the machine actuator was being transferred through the fixtures and thus recorded by the transducers. This problem was not apparent in the old setup which had the AE transducers directly mounted to the test specimen, so the problem had to be with the three point testing fixtures. To reduce this noise, the fixture

design was modified such that polycarbonate was used at the interfaces between the machine and the test fixtures (Appendix A) in order to damp the machine-generated noise component. This new setup has proven equally adept at capturing the acoustic emissions generated during the formation of damage during fatigue testing.

The preliminary testing conducted using the sinusoidal loading regime on beams machined from tibias (see above) were loaded to various initial strain levels. Three of these were loaded to the same initial strain level and were tested until failure. Monitoring the acoustic emissions from these samples we noticed that there were bouts of acoustic emissions that were concomitant with increases in compliance. Prior to the increase in compliance a small number of low energy, low amplitude, and short duration acoustic events occurred. Following the increase in compliance a large number of high energy, high amplitude and long duration acoustic events took place. These results were submitted in the form of an abstract to the Annual Meeting of the Orthopaedic Research Society (see Appendix C).

NOTE: We purchased an upgraded acoustic emission board in November of 2004 which was malfunctioning. The system was returned to the vendor for repair on several occasions to address a variety of issues. Our acoustic emission system was at the vendor site for repairs a total of 120 days over a period of 6 months, which lead to significant delays in our testing process. A letter from the vendor detailing the repairs conducted at the vendor site is included in Appendix F.

Histological Characterization of Damage

In our proposal, we planned to use basic fuchsin to label the microdamage and characterize the various histological parameters such as crack density, crack type, crack orientation, and porosity of the tissue. While the use of basic fuchsin method for detecting and measuring crack properties has been the primary protocol used in the past, recent studies have concluded that an alternative has more to offer (*5-7*). The protocol for staining using basic fuchsin calls for dehydration of the specimen overnight in ethanol and embedding in polymethylmethacrylate (PMMA). The main problem with this technique is that more cracks could form during the dehydration procedure and there is no way to determine the difference between damage that existed prior to testing, damage induced by testing, and the damage that could form due to dehydration. These problems can be overcome using chelating fluorochromes to label microdamage due to their unique ability to stain in such as way that we can determine whether the crack was induced prior or during testing. This method will also increase the sample size and thus the amount of gathered data because each specimen will act as its own control. Therefore we decided to amend our previous proposal of using basic fuchsin and perform our histological characterization of microdamage using other fluorescing agents.

Initially, we planned to stain the samples prior to testing with the agent that has the highest affinity for calcium (alizarin complexone) to label any preexisting microdamage. Following testing the agent with the second highest calcium affinity (calcein) would be used to stain the damage induced due to fatigue loading. Due to limits in our fluorescence microscope, we have been forced to use a different staining sequence. Preliminary examination of calcein and xylenol orange using 'scratch' test method showed that they can easily be differentiated using our current fluorescence microscope setup. A sample of bone was first scratched in the vertical direction and then stained in calcein. Next, the same bone was scratched perpendicular to the first scratch and stained in xylenol orange. Examination under the fluorescence microscope clearly show the two scratches stained differently (Figure 3). We will now stain the specimens with calcein prior to testing and xylenol orange after the testing. The specimens will then be sectioned in both the longitudinal and transverse directions and the histological parameters determined. Each of these chelating agents fluoresces in different wavelength when exposed to epifluorescent light, will enable us to determine the crack growth rates of preexisting microdamage as well as the differences between preexisting, fatigue-induced, and embedding-induced microdamage (which will not be stained at all).

While verification of this method of microdamage labeling is provided in the literature (5-7), is has not yet been reported if the stains and the procedure for their application changes the mechanical properties of bone. The staining procedure specifies that the specimen be placed in a solution of the staining agent and then exposed to a vacuum, forcing the uptake of the stain into the tissue. While this occurs and very low vacuum pressures, we are conducting tests to determine if the mechanical properties are affected by the stain and/or the vacuum exposure. So far, we have only tested samples under monotonic conditions and have found no significant differences ($p < 0.05$) in elastic modulus, fracture stress, yield stress, ultimate stress, fracture strain, yield strain, ultimate strain, resilience, or work to fracture related to the staining process. Data from these initial monotonic tests is available in Appendix E. We are currently in the process of conducting three point bending tests of specimens subjected to a similar treatment to test the effect of these stains on the fatigue performance of bone.

Analysis of Data Obtained

We have obtained data from the preliminary testing of 1) the three- point test fixtures used to induce fatigue damage, 2) the acoustic emission system, and 3) a method of histological staining that will allow us to differentiate whether the microdamage was induced prior to or during fatigue testing. The data analysis methods used for each of these three are detailed below.

Three-point bending tests have been conducted using the sinusoidal loading regime on five beams machined from tibias. These specimens were loaded to failure under a range of maximum loads such that the initial strain that developed was between 0.55%ε and 0.70%ε. The test system records the load, actuator displacement at mid-point of specimen, and gage displacement (external LVDT) at the mid-point of the specimen. Specially designed Matlab (The Mathworks, Inc., Natick, MA) software has been developed that uses the output of the test machine to calculate the compliance data. This code will later be used to monitor the compliance in a real-time manner in conjunction with a secondary computer is attached to the test machine.

The acoustic emission detection, as mentioned previously, has been used in preliminary tests. In the beginning, the software collected information on all acoustic events, regardless of whether they originated from microdamage or somewhere else (i.e. the machine-generated noise). Again, specially designed Matlab software has been developed that is able to filter out the machine generated noise. Since we are using two transducers, any acoustic emission generated by damage formation will be detected by both transducers. The first thing the software does is determine the time difference between consecutive acoustic events. If this time difference was below a minimal level (0.01 μs) and the consecutive events were detected by the two transducers, the acoustic event is kept; otherwise the information on that event is considered noise and discarded. The software is undergoing further development that will provide a variety of information, such as how the amplitude, duration, and number of counts fluctuate with time, as well as the rate of acoustic emission event occurrence.

Using fluorescence microscopic techniques we have been able to identify microdamage in cortical bone specimens (Figure 4). The feasibility of the double labeling technique has been verified through scratch tests. Spare sections of bone were scratched and then stained in calcein. They were then scratched a second time perpendicular to the initial scratch and then stained in xylenol orange. Using the fluorescence microscope, we are able to detect the difference between the scratches (Figure 3). Since calcein has a higher affinity for free calcium (i.e. scratched surface), it binds tightly and is not replaced by the xylenol orange during secondary testing. We concluded that these stains will effectively differentiate between the damage that was present prior to testing and that generated by the testing. Monotonic tensile testing conducted thus far concerning the effect of using these stains would have on the mechanical properties of the bone have indicated that there is no effect, although fatigue testing has not yet been completed.

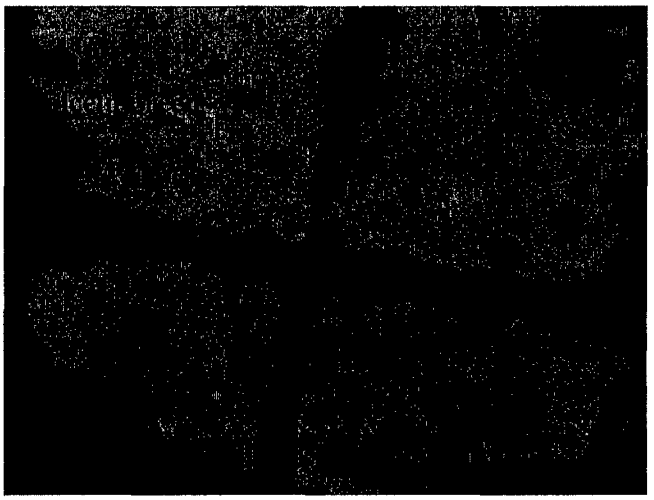

Figure 3: Demonstration of the double staining technique. The orange vertical scratch is calcein green stain and the red horizontal scratch is xylenol orange.

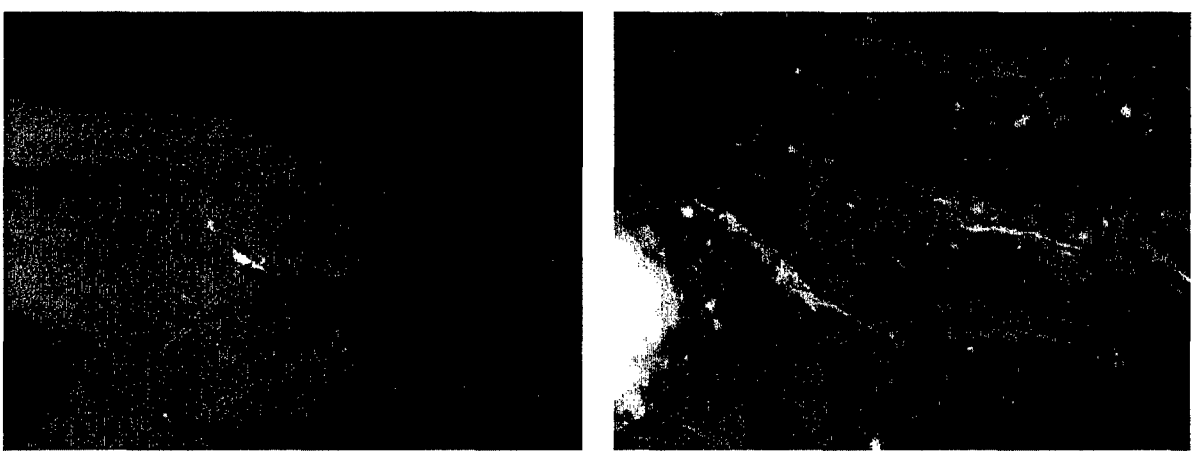

Figure 4: Photographs of bone taken near the fracture surface of specimens tested to failure in tension and stained with calcein. The arrows indicate the fluorescing microcracks.

KEY RESEARCH ACCOMPLISHMENTS

- Acquisition of 27 donor tibias (11 pairs) from which three-point bending test specimens have been/will be machined
- Designed and built a three-point bending apparatus that:
  - Accommodates the specimen size needed for standardized testing
  - Allows the attachment of two acoustic emission transducers to its outer supports
  - Allows specimen displacement monitoring from an external displacement gage
- Developed software that calculated the change in compliance that will later be incorporated as a real-time monitor during the fatigue tests
- Determined acoustic event parameters characteristic of the formation of microdamage

- Verified the capability to detect microdamage using fluorescence microscopy and determine whether the labeled damage occurred prior to, during, and after the fatigue testing sequence
- Conducted preliminary testing to determine the effect of using the more advantageous microcrack staining protocol described above
- Initial monotonic testing indicates no difference in mechanical properties is induced through the staining procedure.
- Have shown the relationship between mechanical property degradation and number of acoustic emission events
- Shown that the energy contents (amplitude, duration, energy) of acoustic emissions vary throughout fatigue testing
- Found that very high energy events took place before the final fracture
- Demonstrated that the acoustic emissions occur in bouts that are immediately followed by a change in the degradation curve

REPORTABLE OUTCOMES

We have conducted preliminary testing of our test setup, including the loading fixture setup, acoustic emission system setup, and verification of a more advantageous histological staining method. One preliminary investigation into the characterization of acoustic events during a fatigue test yielded an abstract that was accepted to the Orthopeadic Research Society's (ORS) 2005 annual conference. The abstract is available in Appendix C, but a brief summary will follow. Four samples of human cortical bone were fatigued at different stress levels in four-point bending in order to induce the formation of microdamage, which was then recorded by the acoustic emission system. We observed that 1) an increase in stress range decreases the fatigue life of the specimen, 2) the compliance, while steady through most of the test, has a sharp increase prior to failure, and 3) a dramatic increase in the number of acoustic emission events detected before the specimen fails. The increase in compliance is well correlated with the increase in acoustic events and it was therefore concluded that an increase in acoustic events can be used to predict the fatigue failure of bone. Also, another preliminary investigation into the effects of loading regime led to another abstract which was submitted for review to the ORS 2006 annual conference (Appendix D). This report showed that 1) damage accumulation occurred in isolated bouts during fatigue, 2) the energy contents of emissions varied throughout the test, and 3) very high energy events took place before the final failure. acoustic emission events are related to the changes seen in the compliance curve such that burst of acoustic emissions are seen prior to changes in the compliance. The results on the effects of fluorochrome stains on bone's mechanical properties are still being collected and we plan to present this work as a technical note for submission to the Journal of Biomechanics.

CONCLUSIONS

We set out with three primary objectives: 1) determine the characteristics of damage events that mark the onset of stress fractures and 2) determine the effect gender on the nature of fatigue damage in bone, and 3) investigate and quantify the damage events during an *in vitro* fatigue of whole bones.

During the first year we focused on the first objective, which consisted of acquiring tibias from human donors, preparing them for testing, develop the test setup including the four-point bending fixtures, loading regimen, monitoring of the acoustic emissions in real-time during the fatigue test, and verification of histological examination techniques.

In the second year, we addressed issues in the test setup and loading regime, the acoustic emission system, as well as the histological examination techniques seen during the first year of the study. We changed our test from a four-point bending to a three-point bending and designed new fixtures for this purpose. Also, an

investigation into the loading regime prompted a change from the high impact loading to a smoother sinusoidal loading method. To address the concern of the easily-damaged acoustic emission transducers, the new test fixture design incorporated new, more rugged transducers and prompted a new approach to acoustic emission data analysis. The histological examination techniques have been modified such that the stains used to label damage have been changed to make the best use of our fluorescence microscope. The change in the microdamage labeling procedure has not been shown to affect the mechanical properties of the samples.

It can be concluded from the work performed in this second year that all the necessary issues have been addressed for us to begin to test specimens. We can perform three-point bending tests that induce fatigue microdamage and we can monitor this microdamage from the acoustic events that its formation generates, and we can successfully use histological staining methods to examine the microdamage following the testing sequence. At receipt of this report, the first set of tests, which will fatigue specimens to failure, will be in progress.

REFERENCES:

1. L. V. Griffin, J. C. Gibeling, V. A. Gibson, R. B. Martin, S. M. Stover, *J Biomech* **30**, 185-8 (Feb, 1997).
2. S. Mori, D. B. Burr, *Bone* **14**, 103-9. (1993).
3. P. Zioupos, J. D. Currey, A. J. Sedman, *Medical Engineering & Physics* **16**, 203-12 (May, 1994).
4. Y. N. Yeni, D. P. Fyhrie, *Bone* **30**, 509-14 (Mar, 2002).
5. T. C. Lee, T. L. Arthur, L. J. Gibson, W. C. Hayes, *J Orthop Res* **18**, 322-5 (Mar, 2000).
6. F. J. O'Brien, D. Taylor, T. C. Lee, *Journal of Biomechanics* **35**, 523-6 (Apr, 2002).
7. F. J. O'Brien, D. Taylor, T. C. Lee, *Journal of Biomechanics* **36**, 973-80 (Jul, 2003).

APPENDIX A: **Fixtures Used for Mechanical Induction of Damage (Three-point Bending)**

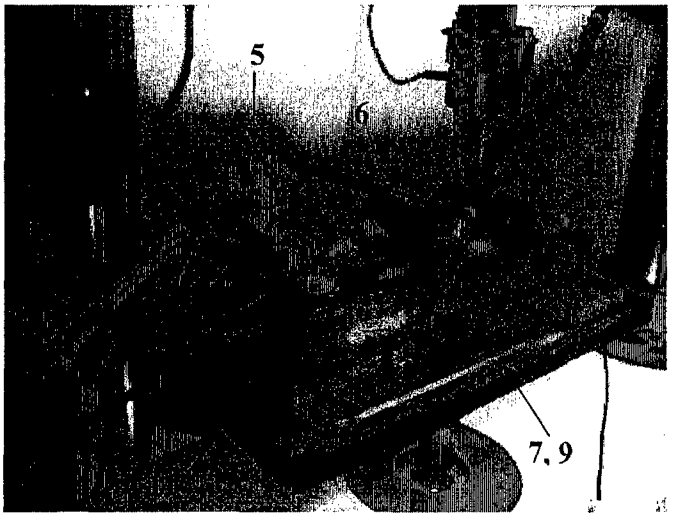

1 Specimen
2 Outer supports (w/ graduated distance markings)
3 Load cell
4 Mid-span loading point
5 Displacement gage
6 AE transducer (only one side pictured)
7 Polycarbonate machine interfaces
8 Solution drip tubes
9 Solution drip pan
10 Solution recirculation pump
11 Solution recirculation tubing
12 Solution reservoir

APPENDIX B: Test group and membership information

Group I : Total Failure			
ID	**Location**	**Age**	**Gender**
ALAM	anterior-medial	22	m
GRAM	anterior-medial	52	m
HLAM	anterior-medial	25	f
ILAM	anterior-medial	48	m
BLAL	lateral	25	m
GRxL	lateral	52	m
IRxL	lateral	48	m
JLAL	lateral	36	m
LLxL	lateral	38	f
PRxL	lateral	19	f
CLLP	posterior	31	f
DLLP	posterior	46	f
FLxP	posterior	22	m
ILxP	posterior	48	m
JRxP	posterior	36	m
ERPM	posterior-medial	49	f
LLPM	posterior-medial	38	f
MRPM	posterior-medial	49	m
NLPM	posterior-medial	22	m
ORPM	posterior-medial	44	m

n = 20

Group II: Pre-Knee			
ID	**Location**	**Age**	**Gender**
BLAM2	anterior-medial	25	m
IRAM	anterior-medial	48	m
KRAM	anterior-medial	24	f
ALxL	lateral	22	m
BLPL	lateral	25	m
ERxL	lateral	49	f
GLPL	lateral	52	m
JLPL	lateral	36	m
KRxL	lateral	24	f
BLLP	posterior	25	m
CLMP	posterior	31	f
ERxP	posterior	49	f
JLxP	posterior	36	m
MRxP	posterior	49	m
ORxP	posterior	44	m
PRxP	posterior	19	f
FLPM	posterior-medial	22	m
GRPM	posterior-medial	52	m
HLPM	posterior-medial	25	f
JRPM	posterior-medial	36	m

n = 20

Group III: Mid-Knee			
ID	**Location**	**Age**	**Gender**
FLAM	anterior-medial	22	m
JLAM2	anterior-medial	36	m
LLAM	anterior-medial	38	f
MRAM	anterior-medial	49	m
DLPL	lateral	46	f
FLxL	lateral	22	m
GLAL	lateral	52	m
HLxL	lateral	25	f
JRxL	lateral	36	m
ORxL	lateral	44	m
ALxP	posterior	22	m
DLMP	posterior	46	f
GLLP	posterior	52	m
HLxP	posterior	25	f
IRxP	posterior	48	m
NLxP	posterior	22	m
BLPM2	posterior-medial	25	m
DLPM	posterior-medial	46	f
GLPM2	posterior-medial	52	m
ILPM	posterior-medial	48	m
PRPM	posterior-medial	19	f

n = 21

Group IV: Post-Knee			
ID	**Location**	**Age**	**Gender**
JRAM	anterior-medial	36	m
NLAM	anterior-medial	22	m
ORAM	anterior-medial	44	m
PRAM	anterior-medial	19	f
CLAL	lateral	31	f
DLAL	lateral	46	f
ILxL	lateral	48	m
MRxL	lateral	49	m
NLXL	lateral	22	m
BLMP	posterior	25	m
GLMP	posterior	52	m
GRxP	posterior	52	m
KRxP	posterior	24	f
LLxP	posterior	38	f
ALPM	posterior-medial	22	m
GLPM1	posterior-medial	52	m
IRPM	posterior-medial	48	m
JLPM2	posterior-medial	36	m
KRPM	posterior-medial	24	f

n = 19

Males				
	# Specimens			
Location	Group I	Group II	Group III	Group IV
a-m	3	2	3	3
p-m	3	3	3	4
lat	4	4	3	3
post	3	4	4	3

Females				
	# Specimens			
Location	Group I	Group II	Group III	Group IV
a-m	1	1	1	1
p-m	2	1	2	1
lat	2	2	2	2
post	2	3	2	2

Males				
	# Specimens			
Decade	Group I	Group II	Group III	Group IV
3rd	4	5	5	4
4th	2	3	2	2
5th	5	4	3	4
6th	2	2	3	3

Females				
	# Specimens			
Decade	Group I	Group II	Group III	Group IV
3rd	2	4	3	3
4th	3	1	1	2
5th	2	2	3	1
6th	0	0	0	0

APPENDIX C: **Abstracted accepted to the Orthopaedic Research Society's Annual Conference (2005)**

ACOUSTIC EMISSION TECHNIQUES CAN PREDICT THE FATIGUE FAILURE OF CORTICAL BONE

+*Wasserman, N; *Korlepara, V; *Akkus, O
+University of Toledo, Toledo, OH
Ozan.Akkus@utoledo.edu

INTRODUCTION

Stress fractures of bone constitute the most serious musculoskeletal overuse injury during military and athletic training (1). The cascade of events prior to the incidence of stress fractures involves the upregulation of bone turnover, amplification of porosity, induction of greater local strains and associated increase in damage activity. Therefore, we propose that it would be possible to diagnose the progression of the failure process by monitoring the microdamage activity. Acoustic emission technique detects the stress waves generated during the formation of microdamage using surface mounted piezoelectric transducers; thus, it is a viable alternative to monitor damage activity (2). More importantly, it is a non destructive and non invasive technique which has the potential to be utilized as an *in vivo* diagnostic tool. In the current study we sought to answer the following questions: 1) can the onset of stress fractures be predicted by monitoring the microdamage activity via acoustic emissions and 2) how soon before the actual failure can be predicted via acoustic emission. This hypothesis was investigated by listening to acoustic emissions released during in vitro fatigue loading of standardized specimens from human femoral cortical bone.

METHODS

Four prismatic beams were machined from the mid- femoral diaphyses of two males (52 and 53 years-old) using a low-speed saw (South Bay Tech). The widths and the thicknesses of beams were machined as allowed by the actual cross-sectional geometry of femurs, resulting in a thickness range of 2.5 mm to 3.3 mm and a width range of 6.5 mm to 7.5 mm. Lengths of beams were kept standard at 70 mm in length. Beams were subjected to fatigue in four point bending with an inner span length of 30 mm and outer span length of 60 mm under continuous irrigation of calcium supplemented saline solution (3). The cyclic loading was conducted under load control and the maximum load varied to create stresses corresponding to 60% to 80% of the yield stress which was obtained from prior monotonic tests of two prismatic beams. The minimum load was kept at $1/10^{th}$ of the maximum load. The loading waveform was triangular with a 0.1 sec long ramp down followed by a 0.1 sec long ramp up at the rate of 2 Hz. The manifestation of damaging events were assessed by calculating the compliance of specimens by dividing the strain range with the stress range as calculated from the load and displacement (as recorded at the loading point) values, respectively.

An acoustic emission transducer (Pico, PAC, NJ) was mounted at the mid-span of the specimens using cyanoacrylate glue. Signal from the transducer was preamplified and acquired at a rate of 2 MHz using a specialized acoustic emission system (AEDSP 32/16, PAC, NJ). The activity of microdamage was assessed by recording the cumulative number of acoustic emission events.

RESULTS

The specimens were loaded in the low-cycle fatigue regime and the number of cycles to failure (N_F) ranged from 600 to 26363 cycles (Table 1). Compliance curves exhibited two temporal stages: a region of stability where the compliance did not change notably and a second stage characterized by a knee region during which the compliance increased rapidly and concluded with failure of the specimen (Figure 1). Concomitant with the initiation of the knee region was an abrupt increase in the cumulative number of acoustic emission events indicating that prefailure events are predominantly highlighted by the microdamage activity.

We have taken the number of cycles at which the rate of accumulation of acoustic emissions begins (N_P) to spike as the cycle at which acoustic emissions predict the onset of failure. The capacity of acoustic emissions to predict failure was calculated in terms of the percentage of specimen's fatigue life, i.e. $(N_P/N_F)*100$. In all specimens precursor acoustic emission events were detected in the range prior to the characteristic knee region and these events were likely to stem from initiation of microdamage.

DISCUSSION

Results of the current study demonstrated that failure of standardized cortical bone specimens can be predicted ahead of time by monitoring the rate of damage accumulation via the acoustic emission technique. The predictive ability of the technique was such that the failure was detected within 78% ±15% of the fatigue life on the average. The current analysis has focused on the rate of accumulation of acoustic emissions only. Acoustic emissions are sinusoidal bursts and further valuable information could be extracted from these bursts such as the duration, amplitude, energy and the frequency content. These waveforms can be classified to identify and extract those bursts which mark the onset of failure (4). Further refinement of the method holds promise for *in vivo* detection of stress fractures in the field using acoustic emissions.

Table 1. The predictive capability of acoustic emissions expressed in terms of the specimen's fatigue life

	Maximum Stress [MPa]	N_F, Fatigue Life [cycles]	N_P, Fracture Onset via AE [cycles]	Predictive Capability [% of Fatigue Life]
Specimen 1	55	26363	22580	85%
Specimen 2	61	35020	33382	95%
Specimen 3	66	4737	2989	63%
Specimen 4	71	600	402	67%

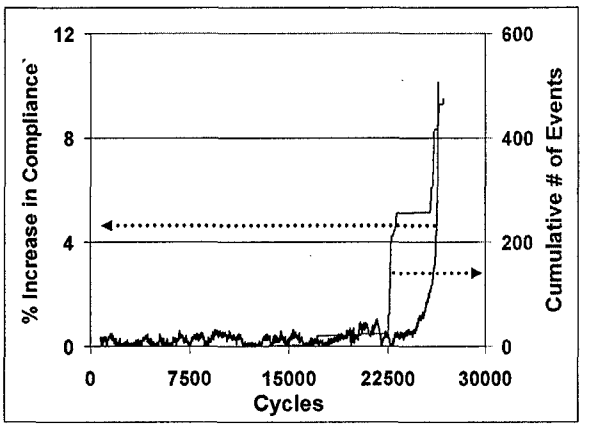

Figure 1. The variation of compliance and the cumulative number of acoustic emission hits with loading cycles.

ACKNOWLEDGEMENTS: This study was funded by the U.S. Army Medical Research and Materiel Command. Tissue was provided, in part, by the Musculoskeletal Transplant Foundation.

REFERENCES: 1) Knapik J et al., 1993 J Occup Med 35:598. 2) Baram J 1993, Experimental Mechanics 33:189-194.3) Gustafson MB, et al., J Biomech 29:1191-4. 1996. 4) Akkus et al., J Mat Sci, 35: 6065-6074.

APPENDIX D: **Abstract submitted to the Orthopaedic Research Society's Annual Conference (2006)**

ENERGETICS OF MICROFAILURE DURING FATIGUE OF HUMAN CORTICAL BONE

*Wasserman, N; +*Akkus, O
+*University of Toledo, Toledo, OH
ozan.akkus@utoledo.edu

INTRODUCTION

Stress fracture of bone is a process which involves generation and propagation of microfailure events. Earlier studies have examined damage accumulation during fatigue testing at different intervals using histology (1). Histology provides substantial insight to damage evolution; however, it is an inherently static process and it can reflect the temporal changes in microfailure processes only by time-consuming histological processing. We have previously shown the ability of acoustic emission (AE, stress wave generated by microfailure events) to predict the impending fatigue failure by simply monitoring the rate of accumulation of acoustic emission events (2). In the current study, we further investigated the energy-based characteristics of microfailure events during fatigue failure of human cortical bone.

MATERIALS & METHODS

Three prismatic beams were machined from the distal diaphysis of tibias from two human donors (31 y.o. female, n = 2 and 1 x 25 y. o. , n = 1 male) using a low-speed saw (South Bay Tech, CA). The widths and the thicknesses of beams were machined as allowed by the actual cross-sectional geometry of femurs, resulting in a thickness range of 1.1 mm to 2.7 mm and a width range of 2.8 mm to 7.2 mm. Lengths of beams were kept standard at 40 mm in length. Beams were subjected to fatigue in three-point bending with a span length of 25 mm and kept under continuous irrigation with calcium supplemented saline solution (3). An initial cyclic loading was conducted within the elastic range in order to determine the initial elastic modulus which was used to calculate the load necessary to create approximately 0.65% strain. Specimens were fatigued under sinusoidal loading with the minimum load corresponding to 10% of the maximum load at a frequency of 2 Hz until failure. The compliance of specimens was calculated from the load and displacement values measured at the mid-span. Compliance is a measure by which one can monitor the overall failure of the specimen and it increases asymptotically towards failure. Acoustic emission (AE) transducers were mounted to the outer supports and the signals associated with AE events were recorded using an AE data acquisition system (Physical Acoustics Corp., NJ). The energetics of microfailure processes were assessed by monitoring the duration, amplitude and energy of recorded AE signals.

RESULTS

The three specimens failed at 9800, 11,800 and 28,000 cycles and the increase in compliance at failure was 25%, 71%, and 126%, respectively. The larger the number of cycles to failure, the larger the number of acoustic emissions were detected (184, 656, 4612, respectively). During the course of fatigue process, acoustic emissions occurred in several bouts each of which were separated by periods of very low AE activity (Fig. 1a). These bouts of AE activity were concomitant with increases in compliance (Fig 1b). Prior to the increase in compliance a small number of low energy, low amplitude, and short duration acoustic events occurred (see circled highlight in Fig. 1b). Following the increase in compliance a large number of high energy, high amplitude and long duration acoustic events took place. The final failure was associated with events whose energy exceeded 35,000 dB-μs, amplitudes exceeding 60 dB, and durations larger than 1000 μs. Once events of these magnitudes were attained, the failure appeared to be imminent.

DISCUSSION

The current study demonstrated three consistent characteristics for accumulation of AE events: 1) damage accumulation occurred in isolated bouts during fatigue, 2) the energy contents of emissions varied throughout the test, and 3) very high energy events took place before the final failure. It is likely that each bout results from induction and growth of microcracks. This growth apparently resulted either in arrest or the growth increment was below the detectable level; thus, leading to periods of relative silence. The low energy, low amplitude, and short duration events prior to increases in compliance (Fig 1b) could arise from incomplete prefailure processes. As the microfailure takes place completely, the compliance increases and higher energy events take place. These observations are in general agreement with previous histological analyses of fatigue damage in bovine bone (1). The future work will use histological analysis of these samples after the occurrence of AE bouts. This way we will be able to associate the energetics of AE events with the physical evidence of damage. This combined approach will shed light on the strength and weaknesses of bone tissue during fatigue and increase our understanding on the material level basis of stress fractures.

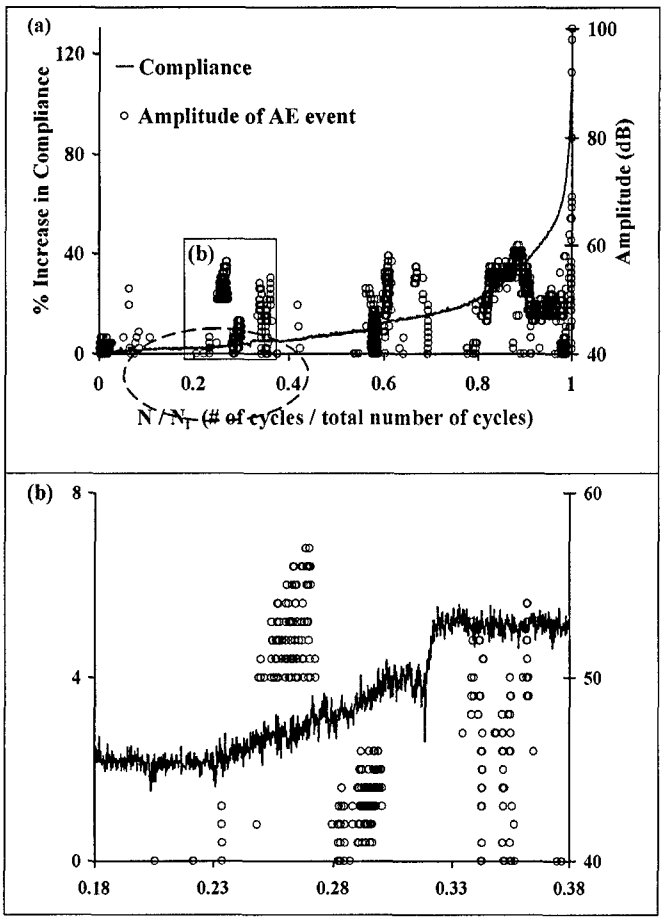

Figure 1: a) Plot of the increase in compliance (left ordinate) and the amplitude of acoustic events (right ordinate) in relation to the normalized number of cycles. Each circle represents one acoustic emission event. b) A close-up view of the inset in 'Fig 1a' where the compliance displaced a local increase.

ACKNOWLEDGEMENTS

We would like to thank the U.S. Army Medical Research and Materiel Command for funding this work.

REFERENCES

(1) O'Brien FJ, et al., J Biomech 36 (2003) 973-980.
(2) Wasserman N, et al., ORS 2005.
(3) Gustafson MB, et al., J Biomech 29 (1996) 1191-1194.

APPENDIX E:

Treatment	Maximum Strain (με)	Yield Strain (με)	Ultimate Stress (MPa)	Fracture Stress (MPa)	Yield Stress (MPa)	Modulus of Elasticity (GPa)	Resilience	Work to Fracture
Ca-Supplemented Solution	0.017 ± 0.007	0.0072 ± 0.0005	91.63 ± 13.17	90.88 ± 13.35	85.73 ± 10.38	16.65 ± 1.30	0.38 ± 0.07	1.34 ± 0.72
Distilled H_2O	0.016 ± 0.004	0.0072 ± 0.0003	94.58 ± 14.23	92.88 ± 15.16	87.61 ± 9.99	17.01 ± 1.90	0.39 ± 0.05	1.26 ± 0.51
Alizarin	0.017 ± 0.005	0.0070 ± 0.0004	92.53 ± 13.98	90.28 ± 12.00	86.80 ± 10.05	17.50 ± 1.86	0.38 ± 0.06	1.29 ± 0.58
Calcein	0.018 ± 0.007	0.0070 ± 0.0003	92.33 ± 17.26	90.25 ± 18.47	85.86 ± 12.06	17.32 ± 1.96	0.38 ± 0.07	1.44 ± 0.82
Significance	$p > 0.05$	$p > 0.05$	$p > 0.05$	$p > 0.05$	$p > 0.05$	$p > 0.05$	$p > 0.05$	$p > 0.05$

APPENDIX F: Letter from Physical Acoustics, Inc.

PHYSICAL ACOUSTICS CORPORATION
A MISTRAS Holdings Company

Mr. Nicholas Wasserman
5051 Nitschke Hall
The University of Toledo
2801 W. Bancroft Street
Toledo, OH 43606

Dear Mr. Wasserman,

As per your request for an explanation of the delays that you have experienced regarding the use of your PAC MISTRAS system, I have compiled the following timeline information. This report contains a brief history of the repairs since my involvement beginning in October 2004 and includes a calculation of the total amount of time the equipment was at PAC for repairs.

Repair History Beginning October 2004

1. 10/29/04 Two preamps were received at PAC for repair. No trouble found.
2. 11/11/04 Four sensors, sensor cables and MISTRAS board received to test as a system. No trouble found.
3. 11/19/04 Quoted MISTRAS controller system to integrate all existing components and test/calibrate as a whole. Received PO to proceed that same day.
4. 12/22/04 Shipped integrated system and all components.

Total time at PAC: 55 days.

5. 12/30/04 UT reported boot problem with new system. PAC recommended re-connecting parts that may have become loose in shipment. UT checked components internally and everything OK.
6. 01/28/05 UT reports intermittent lockups (computer freeze) during AEwin operation. PAC suggested un-installing and re-installing PAC software.
7. 02/03/05 UT reported software reinstallation did not remedy the lockup problem. Returning unit to PAC.
8. 02/08/05 PAC receives unit. Replaces several hardware components and reconfigures Windows and AEwin software.
9. 03/14/05 PAC returns unit to UT.

Total time at PAC: 36 days.

10. 03/15/05 UT reports system failure for exact same type of computer lockup.
11. 03/17/05 PAC receives unit. Replaces more hardware components and reinstalls Window and AEwin software.
12. 04/15/05 PAC returns unit to UT.

Total time at PAC: 29 days.

Grand Total time at PAC for Repairs/Upgrades/Testing/Calibration (10/04-4/05): 120 days.

As of the week of April 18, the unit was reported as operating normally by UT personnel.

If you have questions concerning this matter, please contact me directly.

We apologize for the extraordinary delays that were incurred during the repair and upgrade of this unit. We sincerely commit to provide better service to the University of Toledo in the future.

Cordially,

Donald J. Potts
Customer Service Manager

Physical Acoustics Corporation
195 Clarksville Road
Princeton Junction, NJ 08550
PH: 609-716-4044
FX: 609-716-0706
dpotts@pacndt.com